Proceedings of the Canadian Society for Mechanical Engineering International Congress 2021
CSME Congress 2021
June 27-30, 2021, Charlottetown, PE, Canada

Generating Geometrical Models for Tubular Braided Composites

Ali Gholami[1], Garrett W. Melenka[1*]
[1]Department of Mechanical Engineering, York University, Toronto, Canada
*gmelenka@yorku.ca

Abstract— A program for generating a geometrical model of Tubular Braided Composites is developed in this paper. The MATLAB and SolidWorks software packages are combined for generating the solid model. The step-by-step process for generating different 2D TBC patterns is explained, and the relevant models are shown. The program's output is compared against commercial software and micro-Computed Tomography results.

Keywords- Tubular Braided Composite; Geometrical Model

I. INTRODUCTION

Composite materials constitute two or more materials with different mechanical properties. Combining these materials provides improved mechanical properties that none of them can provide individually [1]. Braided composites are continuous fiber-based reinforced materials used in various industries, from aerospace, automotive, petroleum, and building to medical treatments, sporting and marine [2]–[4]. They can be used in a rope to reinforce hoses and pipes or medical catheters [5]. For more than 200 years, braiding has been used to produce textile fabrics [2]. Braided composites have significant advantages compared to conventional laminate composites, such as better out-of-plane stiffness, strength, toughness properties, net-shape fabrication, lower fabrication cost, impact and delamination resistance, and high performance [6][7]. Because of these advantages, the studies in analyzing and manufacturing braided composite and their application are increasing significantly.

There are different types of braided composite; two-dimensional, three-dimensional, and multidirectional. Each of these types can be produced as flat or tubular shapes. In two-dimensional braided composites, yarns are interlaced only in one plane, and the preform can be manufactured either flat or tubular. Two-dimensional (2D) braided composites can be produced using a Maypole braider. In triaxial two-dimensional braided composite, there are additional yarns interwoven between two-dimensional braids and directed alongside the axial braided composite [8]. One way to categorize 2-D braided composites is based on the assembly pattern of yarns. Depending on the arrangement and movement of carriers, different patterns of braided composites will be made. The patterns of the braided composites are diamond (one tow passing above and then below the other tows, 1/1) Figure 1 a), regular (two tows passing above and then below the other tows, 2/2) Figure 1 b), and Hercules (three tows passing above and then below the other tows 3/3) Figure 1 c).

a)

b)

c)

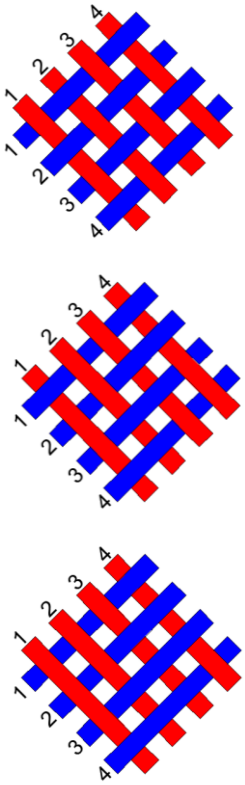

Figure 1 Different pattern of braided composite (a): 2-D Diamond (one by one), (b): 2-D Regular (two by two), (c) 2-D Hercules (three by three)

Tubular Braided Composites (TBC) have several variables, such as variable geometry, variable constituents, and non-uniform feature of braided composites. Thus, the characterization of braided composites is not an easy and straightforward task. However, to optimize the TBC's current application and introduce the new applications, knowing the mechanical properties is paramount. Also, for obtaining mechanical properties of braided composites accurately, more accurate geometrical models are needed. Some of the geometrical variables of a regular braided composite pattern within a unit cell are shown in Figure 2. The shown variables are

braid angle, yarn width, and undulation length. Braid angle is the most important geometrical variable that significantly affects the mechanical properties of the TBC. Other parameters affect the TBC's mechanical properties, such as the radius of the mandrel and the number of yarns, which will be introduced in the following sections.

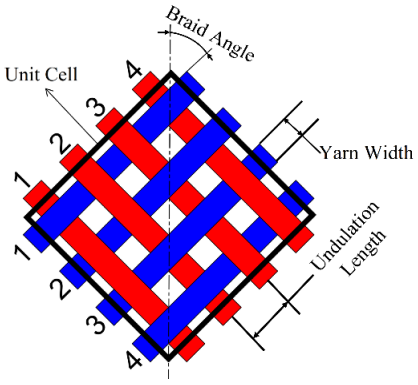

Figure 2 A unit cell of a regular braided composite pattern showing geometrical variables

Several studies have tried to provide more mathematically accurate models for tubular braided composites. Liao and Adanur [9] developed an external and an internal three-dimensional circular braid model. They used the Frenet frame technique for sweeping the cross-section over the yarn path. Rawal and Potluri [10], [11] developed an algorithm to produce three-dimensional braided preforms over different mandrel cross-sections; cylinder, square prism, cones with a circular and elliptical cross-section, and square pyramid. The yarn paths are modelled as straight lines, and undulation is ignored in their model. Alpyildiz [12] proposed a 3-D geometrical model for tubular braids. She considered the braiding yarn's crimp together with the tubular curvature of the tubular braid structure in her model. The provided model worked with different braid structures, braid angle, the number of yarns in a set, yarn, and mandrel diameter. Rawal et al. [13] developed geometrical models in both cylindrical and conical mandrels with diamond, regular and triaxial forms. They used the Virtual Reality Modeling Language (VRML) to simulate the model. Finally, the model was verified against the results of a virtual experiment.

In this paper, a program for designing and illustrating the geometrical model of TBC will be introduced. The developed algorithm can be used as a step for generating a comprehensive geometrical model for future finite element modeling (FEM). Even though the geometrical models are made based on several assumptions which will add errors to the simulation results, having them will make a good benchmark when comparing against other experimental geometrical models like micro-Computed Tomography (μCT).

II. Geometrical Equations

While the geometrical equations need to be as accurate as possible and easy to implement, they should be realistic enough to provide precise models simulating tubular braided composite's actual shape and behavior. However, creating a geometrical model without making assumptions is not possible. For the used geometrical model in this paper, the following assumptions have been made [11]:

- The cross-section of the yarn is assumed to be circular with r radius
- The braid paths do not slip and keep the constant sinusoidal pattern throughout the braid length
- There is no compression on the yarns, so the yarn cross-sections are constant
- The longitudinal yarn in triaxial braided composites are straight

The assumptions mentioned above are considering TBC's overall characteristics; however, they ignore some of the specifications, such as the flexible nature of yarn paths and variant cross-section shapes. For considering these specifications, other methods like μCT, which can provide an actual experimental model, can be used.

Depending on the braided composite pattern, there would be different equations to model them. However, since all the patterns follow a uniform helical path along the mandrel, there would be no difference in different patterns' helical path equations. A left-hand (clockwise from top view) helix's general equations for a yarn path around a cylindrical mandrel are shown in (1).

$$\begin{aligned} X_{cw} &= R\cos\theta \\ Y_{cw} &= R\sin\theta \\ Z_{cw} &= R\theta\cot\alpha \end{aligned} \tag{1}$$

Where X_{cw}, Y_{cw}, and Z_{cw} are coordination points in x, y, and z directions, R is the helix's radius, θ is the winding angle, and α is the braid angle. For having the right-hand (counterclockwise from top view) helical path, the sign of the Y should be changed as shown in (2).

$$\begin{aligned} X_{ccw} &= R\cos\theta \\ Y_{ccw} &= -R\sin\theta \\ Z_{ccw} &= R\theta\cot\alpha \end{aligned} \tag{2}$$

A sample of clockwise and counterclockwise helix path with helix radius (R) = 10 mm, braid angle (α) = 45°, and winding angle (θ) between 0 and 4π, are shown in Figure 3.

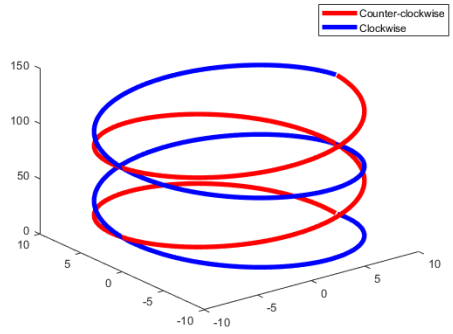

Figure 3 A clockwise and counter-clockwise helix with R = 10 mm, α = 45°, and $0 < \theta \leq 4\pi$

The helix shown in Figure 3 is for two periods (4π). For calculating the height of the helix, one needs to calculate the maximum Z, which in this case it would be $10\,mm \times 4\pi \times \cot 45° = 125.66\,mm$.

On the other hand, each yarn path follows a sinusoidal path based on its braiding pattern. The equation relating the number of yarns, the radius of the strand, and the winding angle to the sinusoidal yarn path is shown in (3) [11].

$$S(\theta) = r \sin\left(\frac{N\theta}{2}\right) \tag{3}$$

Where r is the radius of the yarn and N is the total number of yarns. The undulation path of a sinusoidal path with $r = 0.5\,mm$, $N = 2$, and $0 < \theta \leq 2\pi$ is shown in Figure 4.

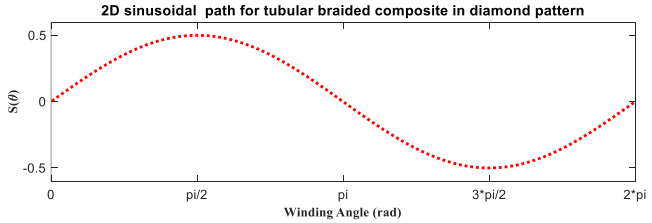

Figure 4 General sinusoidal path of yarn path with $r = 0.5\,mm$, $N = 2$, and $0 < \theta \leq 2\pi$

For a complete set of tubular braided composite, two series of sinusoidal equations are required for counterclockwise and clockwise directions ($S_1(\theta)$ and $S_2(\theta)$). For doing so, a π phase shift should be considered for the equations.

For having the complete yarn path of braided composite, with helix shape and including the undulations, equations (1) and (2) should be mixed with the relevant version of equations (3). By doing so, equations (5) and (6) are created for counterclockwise and clockwise yarn paths, respectively.

$$\begin{aligned} X_i &= \big(R + S_1(\theta)\big)\cos(\theta + (i-1)\beta) && i = 1,2 \ldots n \\ Y_i &= \big(R + S_1(\theta)\big)\sin(\theta + (i-1)\beta) && i = 1,2 \ldots n \\ Z_i &= R\theta \tan\alpha && i = 1,2 \ldots n \end{aligned} \tag{5}$$

$$\begin{aligned} X_i &= \big(R + S_2(\theta)\big)\cos(\theta + (i-1)\beta) && i = 1,2 \ldots n \\ Y_i &= -\big(R + S_2(\theta)\big)\sin(\theta + (i-1)\beta) && i = 1,2 \ldots n \\ Z_i &= R\theta \tan\alpha && i = 1,2 \ldots n \end{aligned} \tag{6}$$

Where n is the total number of yarns at each direction (i.e., $n = N/2$) and β is the shift angle and is calculated as the angle between each two strands (i.e., $\beta = 2\pi/n$). These equations are the same for all patterns of TBC. The only factor making the difference between yarn patterns are $S_1(\theta)$ and $S_2(\theta)$ which will be discussed in the next sections.

A. *Diamond pattern*

The diamond pattern is the most straightforward pattern of the tubular braided composite because the whole path is sinusoidal, and no flat section is incorporated into the path. The $S_1(\theta)$ and $S_2(\theta)$ which are representing counter-clockwise and clockwise sinusoidal paths are as follows:

$$S_1(\theta) = r \sin\left(\frac{N\theta}{2} + \frac{\pi}{2}\right) \tag{7}$$

$$S_2(\theta) = r \sin\left(\frac{N\theta}{2} + \frac{3\pi}{2}\right) \tag{8}$$

A sample of the sinusoidal path of diamond pattern with $r = 0.5\,mm$, $N = 2$, and $0 < \theta \leq 2\pi$ is shown in Figure 5.

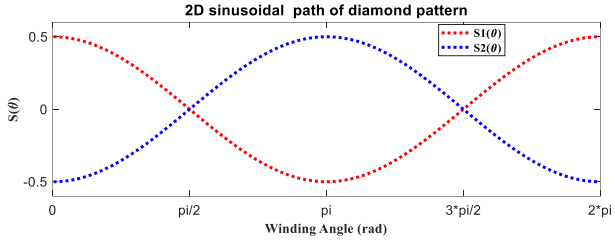

Figure 5 counterclockwise (red) and clockwise (blue) undulation path of diamond pattern

A sample of diamond braided composite yarn path (counterclockwise and clockwise) with pattern and $N = 32$, $R = 10\,mm$, $r = 0.5\,mm$, and $\alpha = 45°$ is shown in Figure 6 (only one of the yarn at each direction is shown for more clarity).

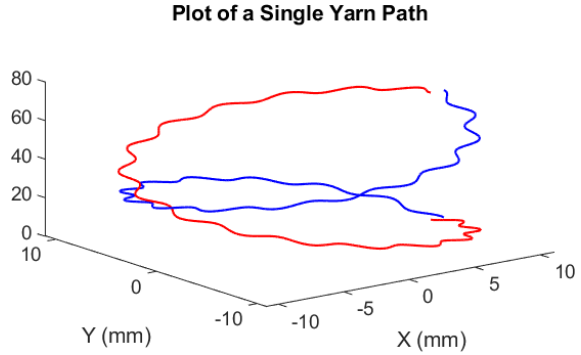

Figure 6 Clockwise (blue) and counterclockwise (red) yarn path of diamond patterns with $N = 32$, $R = 10\,mm$, $r = 0.5\,mm$, and $\alpha = 45°$

B. *Regular pattern*

The shape of the regular pattern is based on the diamond pattern. In the regular pattern, each yarn passes over two yarns moving in the other direction and under two others. Because of that, they involved a flat section for the distance between yarns. The transient area-going from the top of two yarns to the under the two next and vice versa- is still covered by the sinusoidal equations shown in the previous section. A sample of regular yarn path with $r = 0.5\,mm$, $N = 2$, and $0 < \theta \leq 4\pi$ is shown in Figure 7.

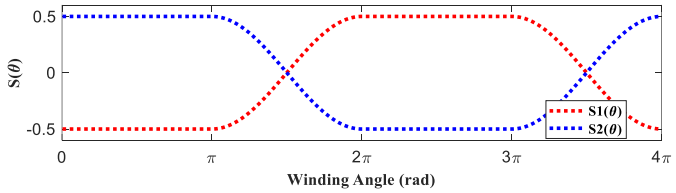

Figure 7 counterclockwise (red) and clockwise (blue) undulation path of regular pattern with $r = 0.5\,mm$, $N = 2$, and $0 < \theta \leq 4\pi$

The counter-clockwise and clockwise equations for the undulation path of the regular pattern are shown in (9) and (10), respectively.

$$S_1(\theta_j) = \begin{cases} r & ;0 \le \theta_j < \beta/2 \\ -r\sin\left(\frac{N\theta_j}{2}+\frac{\pi}{2}\right) & ;\beta/2 \le \theta_j < \beta \\ -r & ;\beta \le \theta_j < 3\beta/2 \\ r\sin\left(\frac{N\theta_j}{2}+\frac{\pi}{2}\right) & ;3\beta/2 \le \theta_j < 2\beta \end{cases} \quad (9)$$

$$S_2(\theta_j) = \begin{cases} -r & ;0 \le \theta_j < \beta/2 \\ -r\sin\left(\frac{N\theta_j}{2}+\frac{3\pi}{2}\right) & ;\beta/2 \le \theta_j < \beta \\ r & ;\beta \le \theta_j < 3\beta/2 \\ r\sin\left(\frac{N\theta_j}{2}+\frac{3\pi}{2}\right) & ;3\beta/2 \le \theta_j < 2\beta \end{cases} \quad (10)$$

Where $j = 0,1,2,\ldots length(\theta)$.

By combining equations (9) and (10) by equations (5) and (6), the yarn path of the regular pattern will be achieved. A sample of braid yarn with a regular pattern, with $N = 16$, $\alpha = 30°$, $R = 10\ mm$, and $r = 0.5\ mm$ is shown in Figure 8 (only one of the yarn at each direction is shown for more clarity).

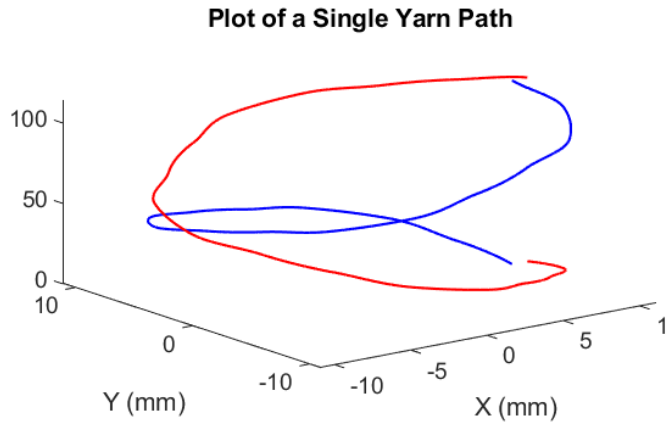

Figure 8 One clockwise (blue) and one counter-clockwise (red) yarn of a designed regular braid with $N = 16$, $\alpha = 30°$, $R = 10\ mm$, and $r = 0.5\ mm$

C. Hercules pattern

Hercules pattern is similar to regular and diamond pattern in terms of the sinusoidal and flat section. However, since in the Hercules pattern, a yarn passes above three yarns and then goes under the next three yarns, the straight section is two times longer than the regular pattern. A sample of counterclockwise and clockwise undulation path of Hercules pattern with $r = 0.5\ mm$, $N = 2$, and $0 < \theta \le 6\pi$ is shown in Figure 9. As one can see, the flat sections are twice longer than the regular pattern. The sinusoidal undulations are the same as regular and diamond patterns.

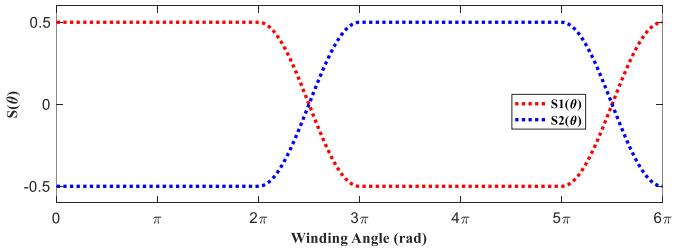

Figure 9 counterclockwise (red) and clockwise (blue) undulation path of Hercules pattern with r=0.5 mm, N=2, and 0<θ≤6π

The counterclockwise and clockwise equations for the Hercules pattern's undulation path are shown in (11) and (12), respectively.

$$S_1(\theta_j) = \begin{cases} r & ;0 \le \theta_j < \beta/2 \\ r & ;\beta/2 \le \theta_j < \beta \\ r\sin\left(\frac{N\theta_j}{2}+\frac{\pi}{2}\right) & ;\beta \le \theta_j < 3\beta/2 \\ -r & ;3\beta/2 \le \theta_j < 2\beta \\ -r & ;2\beta \le \theta_j < 5\beta/2 \\ r\sin\left(\frac{N\theta_j}{2}+\frac{\pi}{2}\right) & ;5\beta/2 \le \theta_j < 3\beta \end{cases} \quad (11)$$

$$S_2(\theta_j) = \begin{cases} -r & ;0 \le \theta_j < \beta/2 \\ -r & ;\beta/2 \le \theta_j < \beta \\ r\sin\left(\frac{N\theta_j}{2}+\frac{3\pi}{2}\right) & ;\beta \le \theta_j < 3\beta/2 \\ r & ;3\beta/2 \le \theta_j < 2\beta \\ r & ;2\beta \le \theta_j < 5\beta/2 \\ r\sin\left(\frac{N\theta_j}{2}+\frac{3\pi}{2}\right) & ;5\beta/2 \le \theta_j < 3\beta \end{cases} \quad (12)$$

Similar to regular pattern equations, by combining equations (11) and (12) by equations (5) and (6), the equations for the Hercules pattern will be achieved. A sample of Hercules pattern with $N = 8$, $\alpha = 60°$, $R = 10\ mm$, and $r = 0.5\ mm$ is shown in Figure 10 (only one of the yarn at each direction is shown for more clarity).

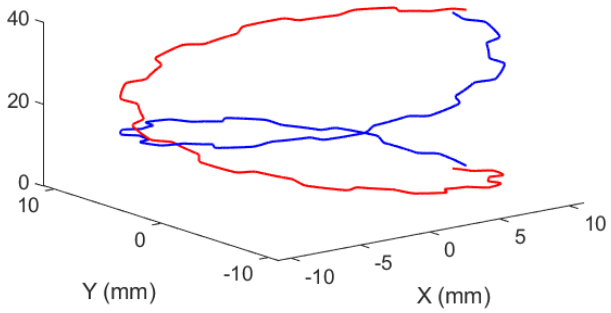

Figure 10 One clockwise (blue) and one counter-clockwise (red) of a designed Hercules braid yarn path with $N = 8$, $\alpha = 60°$, $R = 10\ mm$, and $r = 0.5\ mm$

D. MATLAB algorithms used for generating yarn patterns

The algorithm needed for generating diamond pattern is straight forward. However, special considerations should be taken into account for generating regular and Hercules patterns.

For generating all of the different patterns discussed in the previous sections, a program is designed in the MATLAB software package (R2020B, The MathWorks Inc, Natick, Ma, USA). The program's designed user interface is shown in Figure 11 (a).

The designed program needs five input geometrical variables to design the yarn path. Number of yarns, braid angle (in degree), the diameter of the mandrel in mm (inner diameter of the tubular braid, it should also be considered that the diameter of the mandrel is $2(R-r)$), the diameter of the strand ($2r$) in mm, and the number of turns or height of the tubular braid in mm (only one of these two variables is required to be inputted, the other variable will be calculated based on the inputted value). This program can produce all three yarn patterns, i.e. Diamond, Regular, and Hercules. The user can select to see the single path of clockwise or counterclockwise yarn or both at the same time. As the user changes the parameters, the updated path will automatically be displayed in the plot section. The complete TBC path is displayed in a separated window, as shown in Figure 11 (b). Finally, the XYZ center points of the designed yarn path for counterclockwise and clockwise directions, and a properties file including the input parameters, the designed pattern, and date and time, can be exported as three separated text files by clicking on "Write to .txt file" button. Created clockwise or counterclockwise yarn paths can be uploaded and displayed in the program's display window. The XYZ values are also displayed in the program for control purposes. Alternatively, the generated properties file can be uploaded as well. By uploading the properties file, the program will scan and read the parameters and the pattern of the TBC path and change the program's setting accordingly.

a)

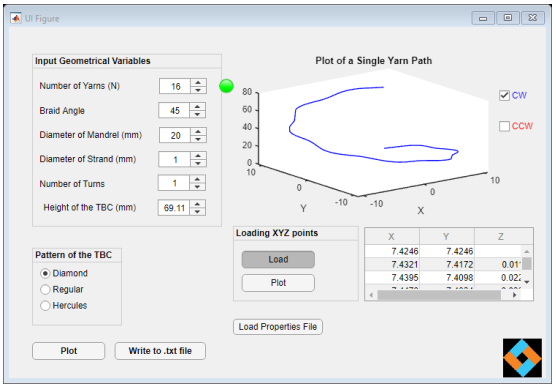

b)

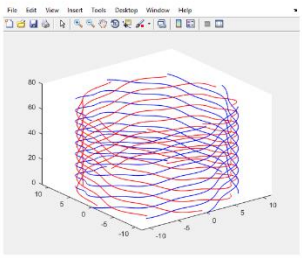

Figure 11 The interface of the developed software for generating yarn path (a), The complete set of clockwise and counterclockwise yarn path (b)

E. Generating the solid geometrical model

For creating the geometrical model by adding a cross-section to the designed yarn path in the previous section, the SolidWorks software (version 2020, Dassault Systèmes SOLIDWORKS Corp., Massachusetts, USA) is used. One clockwise and one counterclockwise yarn path generated in MATLAB is imported into SolidWorks. The generated text file in the developed MATLAB program is imported into the SolidWorks as the "Curve though XYZ Points…" function. After importing both of the yarn paths, two separate circular cross-sections are sketched in the XY plan while the center of the circle coincides with the yarn path. By using the "Sweep" function, the cross-section sweeps the designed path and creates the yarn solid geometrical model. Finally, by using the "Circular Pattern," n number of yarns are patterned around the TBC's axis for each of the counter-clockwise and clockwise directions. A sample TBC solid geometrical model from each pattern is shown in Figure 12. A diamond TBC with $N = 32$, $r = 0.5\ mm$, $R = 10\ mm$, and $\alpha = 45°$ is shown in Figure 12 a), a regular pattern TBC with $N = 36$, $r = 1\ mm$, $R = 15\ mm$, and $\alpha = 45°$ is shown in Figure 12 b); and a Hercules TBC with $N = 64$, $r = 0.5\ mm$, $R = 10\ mm$, and $\alpha = 60°$ is shown in Figure 12 c)

a)

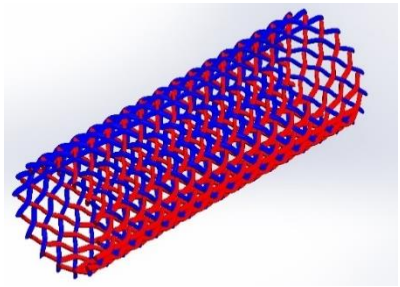

b)

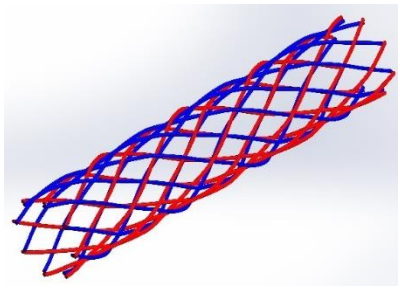

c)

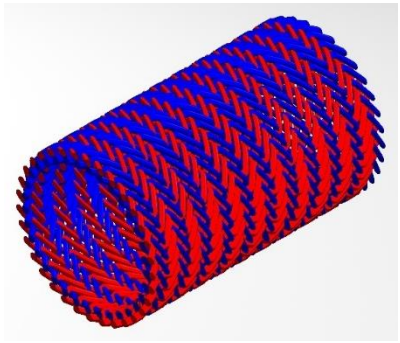

Figure 12 3-D solid model of a TBC, a) Diamond pattern with $N = 32$, $r = 0.5\ mm$, $R = 10\ mm$, and $\alpha = 45°$, b) Regualr with $N = 16$, $r = 0.5\ mm$, $R = 10\ mm$, and $\alpha = 30°$, and c) Hercules with $N = 64$, $r = 0.5\ mm$, $R = 10\ mm$, and $\alpha = 60°$

For validation of the developed model in this paper, a regular TBC with 16 yarns, braid angle = 35°, mandrel radius 10 mm, strand radius = 0.5 mm, and length of the TBC = 98.7 mm is designed in both the developed model in this paper and a commercial software package, TexMind Braided software [14]. The output results of the two software are shown in Figure 13. The visual comparison between the two models shows a good agreement between two models.

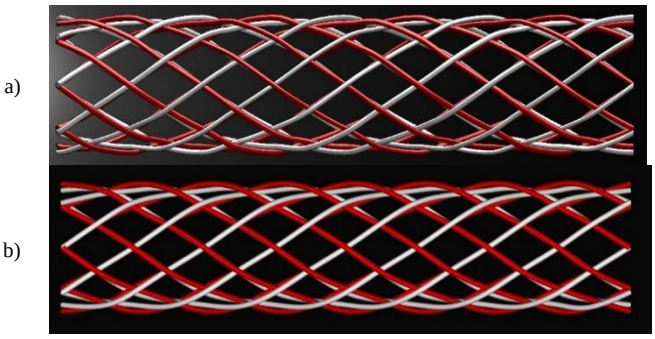

Figure 13 Comparing the result of the generated geometrical TBC model designed by the algorithm developed in this paper a), with the results of the same TBC designed in TexMind Braided software commercial software b). ($N = 16$, α = 35°, R = 10.5 mm, r = 0.5 mm, and the length of the TBC = 98.7 mm)

An actual TBC with the regular pattern is scanned with μCT, and the obtained image is shown in Figure 14 a). The parameters of this TBC are $N = 48$, $r = 0.44\ mm$, $R = 10\ mm$, and $\alpha = 40.53°$. These parameters are used to create the geometrical model of the TBC by using the developed program in this paper, and the resulted image is shown in Figure 14 b). While the braid's overall shape is the same, as seen from the μCT imag in Figure 14 b), some of the yans are not located at their ideal path, and they are distorted significantly. Other assumptions made in generating geometrical equations are adding more errors to it. For quantitative comparison between two models and the amount of error added because of the geometrical model's assumptions, further analysis and required.

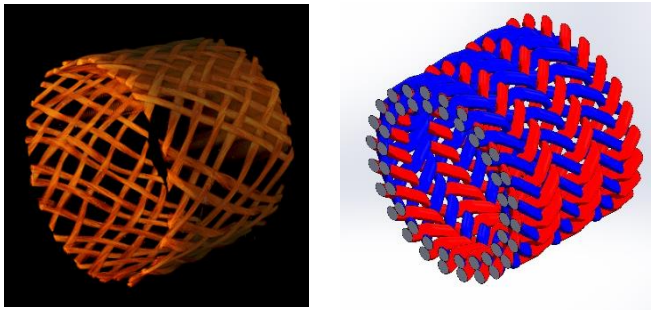

a) b)

Figure 14 Comparison of the actual and simulation model of a regular TBC. a) μCT image of a regular TBC with b) its geometrical model with $N = 48$, $r = 0.44\ mm$, $R = 10\ mm$, and $\alpha = 40.53°$

I. Conclusion

A program for generating TBC's geometrical model was developed in this paper. The MATLAB and SolidWorks were used for generating the geometrical model. The results of this program were compared with the result of another software. Both results were in good accordance. Also, the result of the program was compared against the result of an μCT image of an actual TBC. The error caused by the assumptions made during developing equations was obvious when comparing them.

The generated geometrical model can help the researchers and the industry to have a better understanding of the TBC. This geometrical model can also be used (partially or entirely) to generate Finite Element Models (FEM) to study TBC's behaviour in different conditions. By developing such a simulation model, new applications for TBC will be introduced, and the current applications can be optimized.

II. References

[1] A. K. Kaw, Mechanics of composite materials. CRC press, 2005.

[2] C. Ayranci and J. Carey, "2D braided composites: A review for stiffness critical applications," Compos. Struct., vol. 85, no. 1, pp. 43–58, Sep. 2008, doi: 10.1016/J.COMPSTRUCT.2007.10.004.

[3] G. W. Melenka and J. P. Carey, "Development of a generalized analytical model for tubular braided-architecture composites," J. Compos. Mater., vol. 51, no. 28, pp. 3861–3875, Dec. 2017, doi: 10.1177/0021998317695421.

[4] J. Carey, A. Fahim, and M. Munro, "Design of braided composite cardiovascular catheters based on required axial, flexural, and torsional rigidities," J. Biomed. Mater. Res., vol. 70B, no. 1, pp. 73–81, Jul. 2004, doi: 10.1002/jbm.b.30017.

[5] Y. Kyosev, *Recent developments in braiding and narrow weaving*. 2016.

[6] Z. M. Huang, "The mechanical properties of composites reinforced with woven and braided fabrics," *Compos. Sci. Technol.*, vol. 60, no. 4, pp. 479–498, Mar. 2000, doi: 10.1016/S0266-3538(99)00148-7.

[7] L. Xu, S. J. Kim, C.-H. Ong, and S. K. Ha, "Prediction of material properties of biaxial and triaxial braided textile composites," *J. Compos. Mater.*, vol. 46, no. 18, pp. 2255–2270, Aug. 2012, doi: 10.1177/0021998311431353.

[8] J. P. Carey, *Handbook of advances in braided composite materials: Theory, production, testing and applications*. Woodhead Publishing, 2016.

[9] Tianyi Liao and S. Adanur, "3D Structural Simulation of Tubular Braided Fabrics for Net-Shape Composites," *Text. Res. J.*, vol. 70, no. 4, pp. 297–303, Apr. 2000, doi: 10.1177/004051750007000403.

[10] A. Rawal, P. Potluri, and C. Steele, "Prediction of Yarn Paths in Braided Structures Formed on a Square Pyramid," *J. Ind. Text.*, vol. 36, no. 3, pp. 221–226, Jan. 2007, doi: 10.1177/1528083707072354.

[11] A. Rawal, P. Potluri, and C. Steele, "Geometrical Modeling of the Yarn Paths in Three-dimensional Braided Structures," *J. Ind. Text.*, vol. 35, no. 2, pp. 115–135, Oct. 2005, doi: 10.1177/1528083705057574.

[12] T. Alpyildiz, "3D geometrical modelling of tubular braids," *Text. Res. J.*, vol. 82, no. 5, pp. 443–453, Mar. 2012, doi: 10.1177/0040517511427969.

[13] A. Rawal, S. Gupta, H. Saraswat, and A. Sibal, "Geometrical modeling of near-net shape braided preforms," *Text. Res. J.*, vol. 85, no. 10, pp. 1055–1064, Jun. 2015, doi: 10.1177/0040517514559587.

[14] Y. Kyosev, Y. Kyosev, and Schilgerius, Topology-based modeling of textile structures and their joint assemblies. Springer, 2019.